Available online at www.sciencedirect.com
ScienceDirect
ELSEVIER
Photonics and Nanostructures – Fundamentals and Applications 7 (2009) 47–55
PHOTONICS AND NANOSTRUCTURES
Fundamentals and Applications
www.elsevier.com/locate/photonics

Quantum information processing through quantum dots in slow-light photonic crystal waveguides

C.W. Wong *, J. Gao, J.F. McMillan, F.W. Sun, R. Bose

Center for Integrated Science and Engineering, Solid-State Science and Engineering, and Department of Mechanical Engineering, Columbia University, New York, NY 10027, USA

Received 10 July 2008; received in revised form 10 October 2008; accepted 19 November 2008
Available online 6 December 2008

Abstract

We propose a scheme to realize controlled phase-flip gate between two single photons through a single quantum dot (QD) in a slow-light photonic crystal (PhC) waveguide. Enhanced Purcell factor and large β-factor lead to high gate fidelity over broadband frequencies compared to cavity-assisted system. The excellent physical integration of this PhC waveguide system provides tremendous potential for large-scale quantum information processing. Then we generalize to a multi-atom controlled phase-flip gate based on waveguide system in Sagnac interferometer. Through the Sagnac interferometer, the single photon adds the phase-flip operation on the atomic state without changing the photonic state. The controlled phase-flip gate on the atoms can be successfully constructed with high fidelity in one step, even without detecting the photon.

PACS : 42.70.Qs; 03.67.−a; 42.50.Ct

Keywords: Photonic crystal waveguides; Quantum dots; Sagnac interferometer; Quantum information processing

1. Introduction

Atom-cavity system has been well discussed as the critical components for quantum information processing, such as single photon source [1], two-qubit quantum gate operation [2–3] and entanglement generation [4,5]. Generally optical cavities with high quality factor and small mode volume need to be designed and fabricated to achieve strong coherent interactions between atom and photons. Using a cavity to modify the local density of states (LDOS) is typically limited to a narrow-band spectral region and the photon extraction, scalability and integrability need to be carefully designed. Other possible mesoscopic structures to increase the LDOS include a one-dimensional slow-light photonic crystal (PhC) waveguide [6] or surface plasmons waveguide which has been theoretically proposed recently to create single photon transistors [7]. Remarkable observations in high Q cavities such as enhanced spontaneous emission and strong coupling are also to be expected in the PhC waveguide or nanowire system. Signatures of spontaneous emission enhancement of ensemble quantum dots (QDs) in a PhC waveguide have been demonstrated experimentally [8]. Here we propose a system which consists of PhC waveguides and low-dimensional semiconductor QDs for implementing controlled phase-flip (CPF) gate between two flying qubits. In standard PhC waveguide, a single photon can be reflected by a QD in ground state acting as a nearly

* Corresponding author.
E-mail address: cww2104@columbia.edu (C.W. Wong).

1569-4410/$ – see front matter
doi:10.1016/j.photonics.2008.11.007

perfect mirror, which simultaneously gets a π-phase shift on the reflection. It makes use of tight optical confinement and low group velocity of waveguide modes to influence the emission of a localized QD. Enhanced QDs emission into PhC waveguide mode provides high gate fidelity over broadband frequencies. Excitation of waveguide mode and extraction of QD emission are extremely efficient in this system and "all integration" is possible.

2. Controlled phase-flip gate between two flying qubits in slow-light photonic crystal waveguides

For standard PhC W1 waveguide, the dispersion diagram of fundamental TE-like propagation mode is shown in Fig. 1(a). A divergent-like LDOS and slow group velocity for wavelengths lying near the PhC waveguide cut-off (at 0.266 (c/a) where c is the vacuum speed of light and a is the lattice constant of PhC) are expected with a fundamental propagating waveguide mode. Emission of an emitter embedded in a PhC waveguide (at the field maximum of the localized waveguide mode) exhibits a large spontaneous emission enhancement which is proportional to $(1/v_g V_{eff})$, where v_g is the group velocity and V_{eff} the effective mode volume per unit cell for a PhC waveguide fundamental mode. Furthermore, a large propagation mode β factor (probability of a photon being emitted into a desired waveguide mode regardless of non-radiative decay of the emitter) is obtained throughout the entire propagation spectrum [6]. Fig. 1(b) shows a schematic diagram of the system, with a three-level emitter. Ground and excited states $|g\rangle$ and $|e\rangle$ are coupled via h-polarization photons (corresponding to the waveguide TE mode) with frequency ω_{wg}. A metastable state $|s\rangle$ is decoupled from waveguide modes

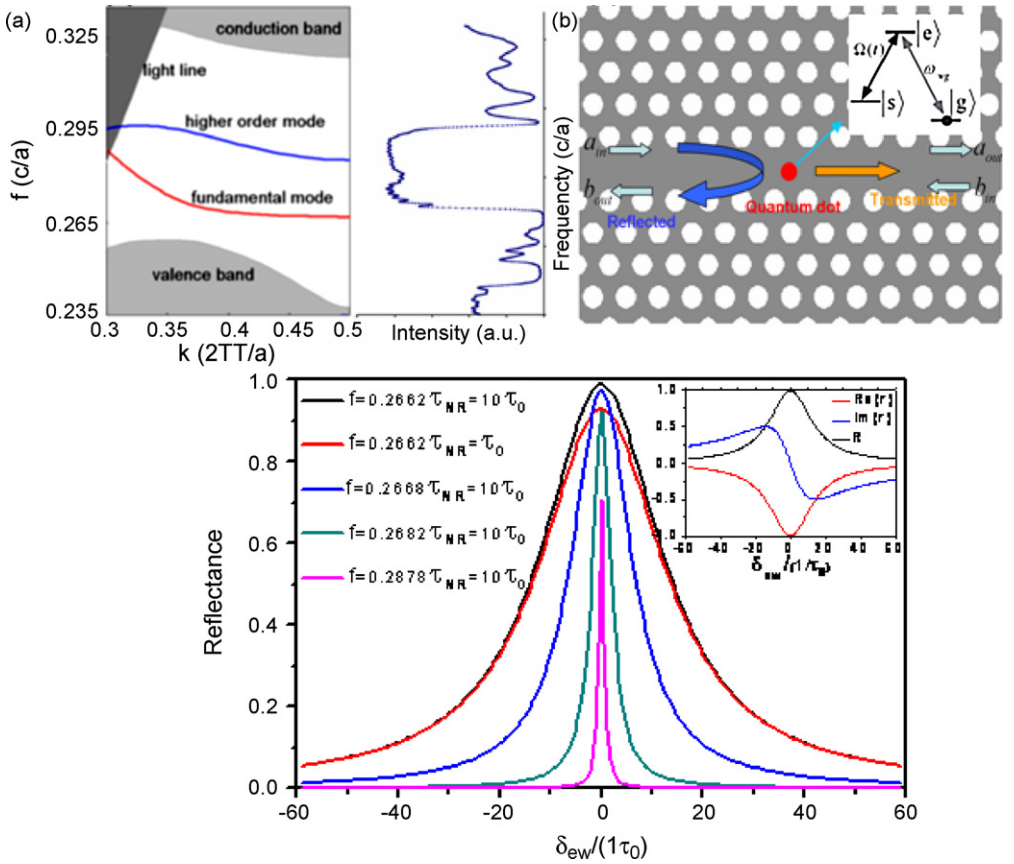

Fig. 1. (a) PhC waveguide band structure within the TE-like band gap. Both fundamental (red) and a higher order mode (blue) are shown. Structure parameters: $r = 0.275a$, $h = 0.5a$, $\varepsilon = 12$ and $a = 420$ nm. Typical transmission spectrum of W1 PhC waveguide is shown on the right panel. (b) Schematic diagram of a single incident photon interacts with a near resonant QD. (c) Reflectance as a function of normalized QD detuning frequencies for different normalized PhC waveguide frequencies with QD $\tau_{NR} = 10\tau_0$ (black, blue, green and pink curves) and $\tau_{NR} = \tau_0$ (red curve). Inset: reflection coefficient (real part and imaginary part) when $f = 0.2662$, $\tau_{NR} = 10\tau_0$. (For interpretation of the references to color in this figure legend, the reader is referred to the web version of the article.)

but is resonantly coupled to $|e\rangle$ via a classical, optical control field with Rabi frequency $\Omega(t)$. Dynamics of the emitter operator σ_- is described by Heisenberg operator equation:

$$\frac{d\sigma_-}{dt} = -\frac{1}{2\tau}\sigma_- + i\delta_{ew}\sigma_- + \kappa a_{in} \quad (1)$$

where a_{in} (b_{in}) is the field operator for the flux of the waveguide input port. The waveguide output fields a_{out} and b_{out} are related to the input fields by $a_{out} = a_{in} + \kappa\sigma_-$ and $b_{out} = b_{in} + \kappa\sigma_-$. $1/\tau = 1/\tau_{SE} + 1/\tau_{NR} + 1/\tau'$ is the total decay rate of the emitter, in which $1/\tau_{SE} = PF/\tau_0$ is the emitter's spontaneous emission rate in PhC waveguide (where PF is the Purcell factor and $1/\tau_0$ is the emitter decay rate in bulk material), $1/\tau_{NR}$ is the non-radiative decay rate and $1/\tau'$ is related to the spontaneous emission into a continuum of radiation and/or leaky modes. δ_{ew} and κ are frequency detuning and coupling coefficient between emitter and waveguide mode respectively, and $\kappa = 1/\sqrt{2\tau_{SE}}$. We use the calculated β factors in Ref. [6] (defined as $\beta = (1/\tau_{SE})/(1/\tau_{SE} + 1/\tau')$ and examined to be greater than 0.9 for perfect polarization match) and consider QD τ_0 = 1 ns and non-radiative decay could be sub-GHz at low temperature [9], Fig. 1(c) shows the reflectance $R = |r|^2 = |b_{out}/a_{in}|^2$ as a function of detuned QDs transition to the normalized frequency of waveguide mode. The waveguide frequencies f are normalized to c/a and are examined for f = 0.2662, 0.2668, 0.2682 and 0.2827. It shows that the reflectance curve gets broader and closer to 1 when the waveguide mode approaches the slower group velocity. The effect of non-radiative emission of QD as a loss mechanism is also shown here in the case of $\tau_{NR} = \tau_0$. The inset shows the reflection coefficient (real part and imaginary part). It indicates that $r \approx -1$ when the QD is on resonance with the waveguide mode with slow group velocity (of $\sim c/154$). An input photon is nearly perfectly reflected by the single QD, and simultaneously gets a π-phase shift. Similar reflection properties are also shown in surface plasmons nanowire [7], and Ref. [10] describes the ideal waveguide case. The existing losses during the photon-emitter interaction come from two aspects: QD dephasing processes and non-unity β factors. We also emphasize the analogy of the reflectance character to that of an unloaded cavity-waveguide system [11], where moving away from the slow-light waveguide edge unloads the coupled QD–PhC waveguide system towards the intrinsic QD linewidth.

Based on the QD–PhC waveguide system we described above, we can adopt Duan's protocol in Ref. [3] to implement a CPF gate by injecting two photons one after the other for several times, together with single qubit rotations. Here we consider a more compact schematic setup as shown in Fig. 2 to realize a CPF gate between two input photon A (target qubit) and B (control qubit). Generally the input photon state A or B can be described as $(|h\rangle + |v\rangle)/\sqrt{2}$ and, after the polarization beam splitter (PBS), only $|h\rangle_A$ mode or $|h\rangle_B$ mode enters at the 50:50 beam splitter (BS) and couples into the PhC waveguide from both sides simultaneously. In PhC waveguide, the single photon state is a superposition of the left- and right-propagation waveguide mode. After traveling through the Sagnac loop, the photon recombines at the BS and comes out from the same port it entered. Moreover, using the 50:50 BS transformation matrix [12], it is known that $|h\rangle_A$ mode and $|h\rangle_B$ mode will gain a π-phase difference with respect to each other when they leave the Sagnac loop and we denote this effect as $|h\rangle_A \xrightarrow{\text{Sagnac}} |h\rangle_A$, $|h\rangle_B \xrightarrow{\text{Sagnac}} -|h\rangle_B$. We note that the optical paths and propagation loss for $|h\rangle$ and $|v\rangle$ components can be stably tuned experimentally to be identical. All these free space light paths can also be integrated onto a single chip. When the emitter is on ground state, $|h\rangle_A$ coming from port A will get a π-

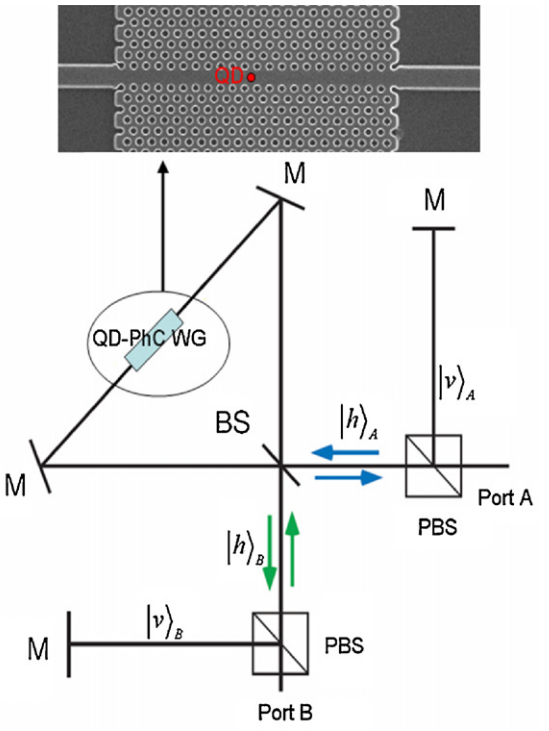

Fig. 2. Schematic setup of CPF gate with Sagnac loop. Photon A (B) enters from Port A (B) and the h-polarized component (after passing the PBS) interacts with single QD positioned in the PhC waveguide.

phase shift after reflecting by QD and leaves our system as $-|h\rangle_A$.

The implementation of CPF gate between photon A and B consists of three steps, and first we show initial and final states of the QD-photon system in the following description to illustrate the states evolution after each step in ideal case:

(I) First we initialize the emitter in ground state and apply a control field $\Omega(t)$ simultaneous with the arrival of single photon B. The control field (properly choose to be impedance matched [13]) will result in capture of the incoming single photon (using $|vac\rangle_B$ to describe h-polarized B photon after storage) while inducing QD state flips from $|g\rangle$ to $|s\rangle$:

$$|h\rangle_B|g\rangle_{QD} \rightarrow |vac\rangle_B|s\rangle_{QD},$$
$$|v\rangle_B|g\rangle_{QD} \rightarrow |v\rangle_B|g\rangle_{QD} \quad (2)$$

(II) Next we send photon A into the system at this time. Only when emitter is on ground state $|g\rangle$, QD-waveguide system will reflect photon $|h\rangle_A$ and introduce a π-phase shift on this photon simultaneously. The reflected photon will finally leave from port A as below:

$$|h\rangle_A|vac\rangle_B|s\rangle_{QD} \rightarrow |h\rangle_A|vac\rangle_B|s\rangle_{QD},$$
$$|v\rangle_A|vac\rangle_B|s\rangle_{QD} \rightarrow |v\rangle_A|vac\rangle_B|s\rangle_{QD},$$
$$|h\rangle_A|v\rangle_B|g\rangle_{QD} \rightarrow -|h\rangle_A|v\rangle_B|g\rangle_{QD},$$
$$|v\rangle_A|v\rangle_B|g\rangle_{QD} \rightarrow |v\rangle_A|v\rangle_B|g\rangle_{QD} \quad (3)$$

(III) Finally we can choose the same $\Omega(t)$ to drive the emitter from $|s\rangle$ back to $|g\rangle$, and retrieve single photon $|h\rangle_B$ as a time reversal process of (I). The retrieval process can be expressed as $|vac\rangle_B|s\rangle_{QD} \rightarrow |h\rangle_B|g\rangle_{QD}$. The retrieval photon generated in PhC waveguide is exactly the same as the input photon in (I), but it will get a π-phase change when it leaves the BS:

$$|h\rangle_A|vac\rangle_B|s\rangle_{QD} \rightarrow -|h\rangle_A|h\rangle_B|g\rangle_{QD},$$
$$|v\rangle_A|vac\rangle_B|s\rangle_{QD} \rightarrow -|v\rangle_A|h\rangle_B|g\rangle_{QD},$$
$$-|h\rangle_A|v\rangle_B|g\rangle_{QD} \rightarrow -|h\rangle_A|v\rangle_B|g\rangle_{QD},$$
$$|v\rangle_A|v\rangle_B|g\rangle_{QD} \rightarrow |v\rangle_A|v\rangle_B|g\rangle_{QD} \quad (4)$$

After these three steps, we have thus achieved:

$$|\varphi\rangle_{initial} = |h\rangle_A|h_B\rangle + |v\rangle_A|h\rangle_B + |h\rangle_A|v\rangle_B + |v\rangle_A|v\rangle_B$$
$$\Rightarrow |\varphi\rangle_{ideal} = -|h\rangle_A|h\rangle_B - |v\rangle_A|h\rangle_B - |h\rangle_A|v\rangle_B + |v\rangle_A|v\rangle_B \quad (5)$$

This ideal photon states evolution demonstrates the successful implementation of controlled phase-flip gate operation, which preserves the final phase of A and B photons relative to input only when they are both in v polarization, otherwise the final phase will get a π-phase change. The emitter will go back to original ground state after the gate operation.

We emphasize the importance of the Sagnac loop in our scheme. Because the PhC waveguide is a two-side coupling system (QD emission couples into both left- and right-propagation waveguide modes), if we have incident $|h\rangle_A$ mode only from one side of the waveguide in step (II) (the QD state at the end of step (I) can be $|g\rangle$ or $|s\rangle$), we will get both transmitted and reflected modes. We cannot combine these two modes later into a single output without loss because they are entangled with the QD. The advantage of using Sagnac loop here is to remove the entanglement between the waveguide left- and right-propagating modes and QD by having $|h\rangle_A$ mode incident from both sides of the waveguide. Thus we can get single output $-|h\rangle_A$ (when QD state is $|g\rangle$) or $|h\rangle_A$ (when QD state is $|s\rangle$).

Furthermore we discuss the storage and retrieval process in steps (I) and (III). We need coherent storage and retrieval of a single photon $|h\rangle_B$ and the store/retrieval efficiency degrades the quality of the control phase gate. In our case, the optimal storage strategy in (I) is splitting the incoming pulse and having it incident from both sides of the emitter simultaneously, which is the time reversal process of a single photon generation. There is a one-to-one correspondence between the incoming pulse shape and the optimal field $\Omega(t)$. The retrieval process in (III) is time-reversal process of the storage process in (I) and both efficiencies are theoretically determined by the calculated reflection/transmission coefficient [7,14]. Reversible transfer of coherent light to and from the internal state of a single trapped atom in a cavity has already been demonstrated in experiment already [15] and the efficiency could improve up to 90%.

Next we consider non-ideal cases which include frequency mismatch between emitter and waveguide mode, non-radiative decay of the emitter, and experimentally achievable values of low group velocities, as well as photon storage and retrieval efficiency. We include all the above loss mechanisms and experimental limitations into the photon loss during the gate operation in Fig. 3(a). Not surprisingly the gate loss decreases to very low level when we operate at the slow-light PhC waveguide frequencies and the gate loss increases when the non-radiative decay of the QD is comparable to the radiative decay. Gate fidelity of the

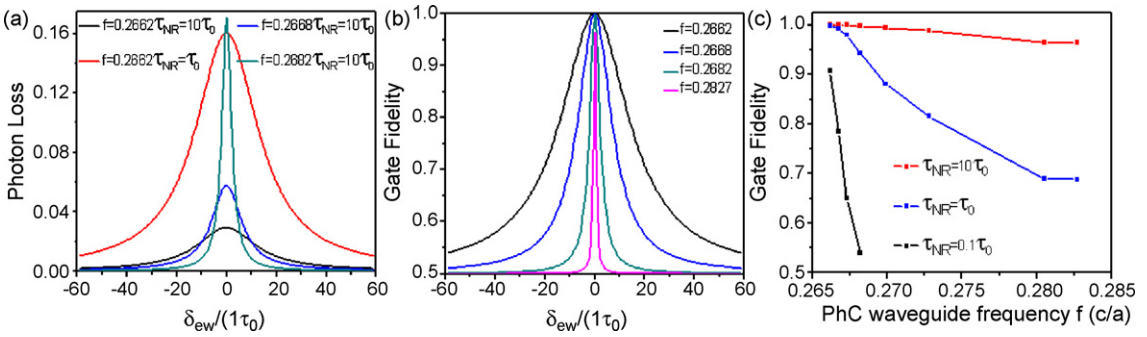

Fig. 3. (a) Gate photon loss as a function of normalized QD detuning frequencies for CPF gate operated at different PhC waveguide frequencies with QD $\tau_{NR} = 10\tau_0$ (black, blue and green curves) and $\tau_{NR} = \tau_0$ (red curve). (b) Gate fidelity as a function of QD detuning frequencies for CPF gate operated at different PhC waveguide frequencies ($\tau_{NR} = 10\tau_0$). (c) CPF gate fidelity as a function of normalized PhC waveguide frequencies with QDs $\tau_{NR} = 10\tau_0$ (red curve), $\tau_{NR} = \tau_0$ (blue curve) and $\tau_{NR} = 0.1\tau_0$ (black curve). (For interpretation of the references to color in this figure legend, the reader is referred to the web version of the article.)

CPF gate, which describes the difference between the actual output photon state and the ideal case in Eq. (5), is an important measurement of the quality of the scheme. We note that the PhC waveguide mode propagation loss and the insertion loss (when light is coupled into and extracted from PhC waveguide) do *not* decrease the gate fidelity. Fig. 3(b) shows the QD-waveguide CPF gate fidelity as a function of normalized QD frequency detuning for the gate operation at different waveguide mode frequencies. In Fig. 3(b) the quick decrease of the gate fidelity also indicates that we always need to match the input photon frequency (waveguide mode frequency) to be on-resonant with the QD transition, although the on-resonance case suffers more gate loss than the off-resonance case (as shown in Fig. 3(a)). We emphasize that the frequency matching here is not as stringent as the cavity cases because of the broad spectral range of the propagating PhC waveguide mode. Fig. 3(c) show the QD-waveguide CPF gate fidelity as a function of PhC waveguide mode frequencies (on resonance with QD) when using QDs with different quantum yields. When $f = 0.2662$, $v_g \approx c/154$ have been measured experimentally [16]. Spontaneous emission rate is enhanced by PF = 30 and leads to β factor nearly 0.998 for a QD located at the field antinodes with the same dipole orientation as the mode polarization [6]. The reflectance peak is as high as 0.988 and leads to gate fidelity up to 0.9999 with $\tau_{NR} = 10\tau_0$ used in the simulations. When $f = 0.2827$, the PF tends towards 1 with normal waveguide group velocity yet gate fidelity remains above 0.96. Although the Purcell factor is very low in this case, the reason of the high fidelity is that the QD emission into free space or other leaky modes are highly suppressed inside the PhC band gap and the one-dimensional waveguide, and thus we have large β factor (>0.9) all through the waveguide mode spectral range ($\sim$10 THz from Fig. 1(a)). Compared with cavity-assisted schemes in which Lorentzian shape resonance features are involved, the gate operation bandwidth in waveguide-assisted system is much larger. For example, as long as the QD transition is within $\sim$2 THz (15 nm) above the waveguide cut-off frequency, our scheme always gets fidelity greater than 0.99 as well as gate loss smaller than 0.18. Even with a QD with 50% quantum yield ($\tau_{NR} = \tau_0$), the gate fidelity still remain higher than 0.9 within $\sim$2 THz frequency range because of the Purcell-enhanced QD spontaneous emission rate into the waveguide mode. For QDs with low quantum efficiency, the gate fidelity stays above 90% only when we operate close to the slow-light edge, and obviously decreases quickly. In this case, schemes with ultrahigh Q cavities will benefit from the larger Purcell factors, reducing the effect of QD's non-radiative decay, but at the expense of cavity-limited bandwidth. Combining the contribution both from Purcell factor and large β factor, our QD–PhC waveguide system has a distinctive advantage compared to cavity-assisted schemes by relaxing the frequency matching condition (frequency match between QD transition and cavity resonance) by $\sim$ two-orders of magnitude or more. We can also take advantage of this broad bandwidth to offset the actual experimental slow-light propagation and coupling losses by operating slightly away from the slowest group velocity regions for acceptable gate fidelity and gate loss.

3. Scalable multi-atom controlled phase-flip gate in slow-light photonic crystal waveguides

Furthermore, we extend and general the previous scheme to construct a multi-atom CPF gate based on the

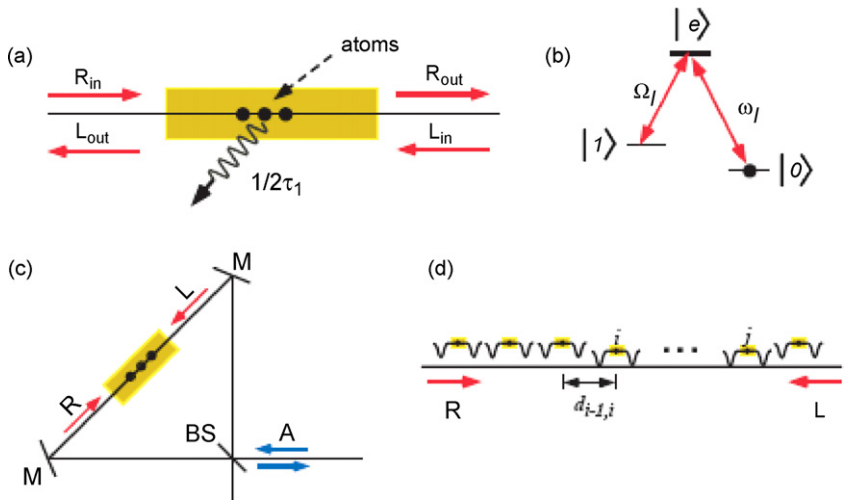

Fig. 4. Schematic illustrations (a) atoms embedded in one-dimensional waveguide system. *R* and *L* are the two counter-propagating modes. (b) Three-level system for each atom examined in our study. (c) Schematic setup to implement the CPF gate among atoms in the Sagnac interferometer. The single-photon is coupled into mode *A* of the beam splitter. After interaction with the atoms, the photon leaves the Sagnac interferometer in mode A without any entanglement with the atoms. (d) Scalability of CPF among arbitrary atoms by external and deterministic control of coupling of each atom-waveguide subsystem to a main bus waveguide. Each represented *i*th subsystem consists of a three-level atom embedded in the one-dimensional waveguide.

one-dimensional waveguide in the Sagnac interferometer. We emphasize that the superposition of the two propagation modes from both sides erases the entanglement between photons and atoms. Without entanglement with the photonic state, the desired atomic state can be achieved with 100% success probability in only *one* step.

In the interaction of the isolated single three-level atom embedded in one-dimensional waveguide, the single photon scattering properties are strongly dependent on the atomic state. As shown in Fig. 4(b), the Λ-type atoms have a ground state $|0\rangle$, an excited state $|e\rangle$, with a metastable state $|1\rangle$. The atomic transition between states $|0\rangle$ and $|e\rangle$ (with frequency ω) is coupled to single photons with frequency υ. There are two guided modes (R and L) in the waveguide for modes propagating to the right and to the left respectively. In the rotating frame approximation, the Hamiltonian of the system containing a single photon and N atoms embedded in a one-dimensional waveguide is

$$H = \sum_k \int_{-\infty}^{\infty} \upsilon \mathrm{d}\upsilon \cdot a_k^\dagger a_k + \sum_l \frac{1}{2}\omega_l \sigma_z^l - i\sum_l \frac{1}{2\tau_l}|e\rangle_{ll}\langle e| + i\sum_{k,l}\int_{-\infty}^{\infty} \mathrm{d}\upsilon \cdot (g_{l,k} a_k^\dagger \sigma_-^l - g_{l,k}^* \sigma_+^l a_k) \tag{6}$$

where $k = R, L$ are for the two optical modes and l are for the different atoms. $1/2\tau_l$ describes the atomic decay of the lth atom into the other modes during the interaction. We normalize to $\hbar = 1$ and assume for simplicity that the interactions between the two modes and single atom have the same coupling constant $g_{l,k} = g_l$. $a^\dagger$ and a are the photon creation and annihilation operators respectively, and $\sigma_+ = |e\rangle\langle 0|$ and $\sigma_- = |0\rangle\langle e|$ are the atomic raising and lowering operators, with $\sigma_z = |e\rangle\langle e| - |0\rangle\langle 0|$. Therefore the Heisenberg equations of motion for photonic and atomic operators are [17]:

$$\dot{a}_k = -i\upsilon a_k + \sum_l g_l \sigma_-^l \dot{\sigma}_l^- = -\left(i\omega_l + \frac{1}{2\tau_l}\right)\sigma_-^l + \sum_k \int_{-\infty}^{\infty} \mathrm{d}\upsilon \cdot g_l^* \sigma_z^l a_k \tag{7}$$

The photonic input and output operators can be defined as $a_k^{\mathrm{in}} = \frac{1}{\sqrt{2\pi}}\int_{-\infty}^{\infty} \mathrm{d}\upsilon \cdot e^{-i\upsilon(t-t_0)} a_{k0}(\upsilon)$ and $a_k^{\mathrm{out}} = \frac{1}{\sqrt{2\pi}}\int_{-\infty}^{\infty} \mathrm{d}\upsilon \cdot e_{k1}^{-i\upsilon(t-t_1)} a_{k1}(\upsilon)$, where $a_{k0}(\upsilon)$ $[a_{k1}(\upsilon)]$ is the value of $a_k(\upsilon)$ at $t = t_0$ ($t = t_1$, $t_1 > t_0$) [17]. Therefore the relation between the photonic and atomic operators have the below motional forms:

$$\dot{\sigma}_l^- = -\left(i\omega_l + \frac{1}{2\tau_l}\right)\sigma_-^l - \sqrt{2\pi}\sum_k g_l^* \sigma_z^l a_k^{\mathrm{in}} + \frac{1}{2}\sum_{k,l'} 2\pi g_l^* g_{l'} \sigma_z^l \sigma_-^{l'} \text{ and } a_k^{\mathrm{out}} - a_k^{\mathrm{in}} = -\sum_l g_l \sigma_-^l \tag{8}$$

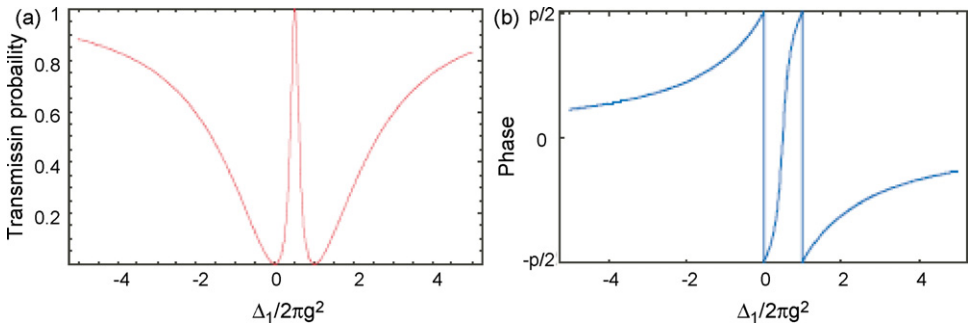

Fig. 5. Transmission transparency in interaction between single-photon and two atoms in a one-dimensional waveguide. (a) Transmission probability for different detunings and (b) phase imposed on the transmitting mode.

In the weak-excitation interaction limit (by a weak monochromatic field or a single photon pulse), the atom is predominantly in the ground state. In this case, $\langle \sigma_z^l \rangle \approx -1$ for all t, and we can set $\sigma_z^l = -1$ [4]. Here we define $P_l(\Delta_l) = 2\pi i|g_l|^2/(\Delta_l + (i/2\tau_l))$ and $P = \sum_l P$. The detuning $\Delta_l = \upsilon - \omega_l$ and $P_l(0)$ is the effective Purcell factor for the resonant cases as defined in Ref. [18]. Therefore, with the method of Fourier transform [17], the input and output mode has the simple relationship:

$$a_{R(L)}^{\text{out}} = \frac{a_{R(L)}^{\text{in}} - P a_{L(R)}^{\text{in}}}{1+P} \tag{9}$$

For case of complete resonance case (all atoms with the same transition frequency ω and $\upsilon - \omega = 0$) and for $2\pi\sum_l |g_l|^2 \gg 1/2\tau$, we have $P >> 1$ and hence the single photon will be reflected in the waveguide by the atoms with a π-phase shift $a_{R(L)}^{\text{out}} \approx -a_{L(R)}^{\text{in}}$.

The result of interaction between the single photon and the single atom has been shown in Fig. 1(c), and also in Ref. [7,10,19]. For the single photon and N atoms case, the above-described enhanced effective Purcell factor $P = \sum_l P_l$ illustrates the coherent superposition of the interactions. For small atomic decay $1/2\tau \to 0$, an analogy to electromagnetically induced transparency appears in the transmission when there is a small but finite detuning between the atomic transition frequencies. Fig. 5 shows the result of the interaction between the single photon and two detuned atoms with $\omega_2 - \omega_1 = 2\pi g^2$. We assume that $|g_1| = |g_2| = g$. The transmission probability and corresponding phase imposed on the transmitting modes are shown in Fig. 5(a) and (b), respectively. In this transmission transparency window, the propagating mode shows slow group velocity [19]. With smaller detuning between the two atomic transition frequencies, the transparency linewidths and group velocities are smaller.

Based on the single-photon's input and output relationship after the atom interactions, the CPF gate can be constructed in only one step in the Sagnac interferometer, as shown in Fig. 4. From the above described scattering properties, when all the atoms are in state $|1\rangle$, the photon does not couple to the atoms and will transmit through the waveguide: $|R_{\text{in}}\rangle(|L_{\text{in}}\rangle) \to |R_{\text{out}}\rangle(|L_{\text{out}}\rangle)$. When there is at least one atom in state $|0\rangle$, the single-photon will be reflected with a π-phase shift $|R_{\text{in}}\rangle(|L_{\text{in}}\rangle) \to -|L_{\text{out}}\rangle(|R_{\text{out}}\rangle)$. However, if the atoms are in the superposition of state $|0\rangle$ and $|1\rangle$, there is entanglement between the atoms and the photon when the photon is incident from only one of the two waveguide modes. For example, the single atomic state $(\alpha|0\rangle + \beta|1\rangle)$ and photon state from in right-input mode $|R_{\text{in}}\rangle$ will have the transformation $(\alpha|0\rangle + \beta|1\rangle)|R_{\text{in}}\rangle \to -\alpha|0\rangle|L_{\text{out}}\rangle + \beta|1\rangle|R_{\text{out}}\rangle$, with a resulting entangled state. However, the entanglement can be erased successfully by superposing the single-photon input in the other mode at the same time. If the input photonic state is $(|R_{\text{in}}\rangle + |L_{\text{in}}\rangle)/\sqrt{2}$, the transformation will be $(\alpha|0\rangle+\beta|1\rangle)(|R_{\text{in}}\rangle+|L_{\text{in}}\rangle)/\sqrt{2} \to (-\alpha|0\rangle+\beta|1\rangle)(|R_{\text{out}}\rangle+|L_{\text{out}}\rangle)/\sqrt{2}$. There is a π-phase change in atomic state $|0\rangle$ *without* any entanglement between atomic state and photonic state. The photonic superposition state $(|R_{\text{in}}\rangle + |L_{\text{in}}\rangle)/\sqrt{2}$ can be easily generated by the symmetric beam splitter in the Sagnac interferometer, and the optical path in both propagating and counter-propagating arms of the interferometer can be easily controlled to be stable in experimental. Correspondingly, the result of interaction between the input photonic state and N atomic states can be simply described as

$$|111,..,1\rangle(|R_{\text{in}}\rangle + |L_{\text{in}}\rangle)/\sqrt{2} \to |111,..,1\rangle \times (|R_{\text{out}}\rangle + |L_{\text{out}}\rangle)/\sqrt{2} \tag{10}$$

$$|\text{atom}_0\rangle(|R_{\text{in}}\rangle + |L_{\text{in}}\rangle)/\sqrt{2} \to -|\text{atom}_0\rangle \times (|R_{\text{out}}\rangle + |L_{\text{out}}\rangle)/\sqrt{2} \tag{11}$$

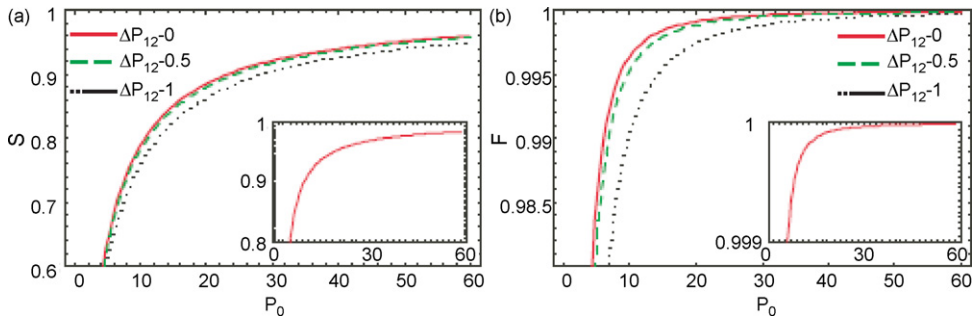

Fig. 6. Illustration of (a) success probability and (b) fidelity of two-atom CPF gate for different effective Purcell factor and ΔP_{12}. ΔP_{12} is the difference of two effective Purcell factors: $\Delta P_{12} = |P_1 - P_2|/P_0$ and $P_0 = (P_1 + P_2)/2$. The insets are the properties of the CPF gate for 10 atoms with the same effective Purcell factor P_0.

where $|111,..,1\rangle$ are for all atoms in state $|1\rangle$ and the $|\text{atom}_0\rangle$ describes the N-atom state with at least one atom in state $|0\rangle$. The photon in the two output modes will be recombined at the beam splitter and leave the Sagnac interferometer in the output port A without being entangled with the atoms. Regardless of the whole phase, the multi-atom CPF gate $U_{\text{CPF}} = e^{i\pi|111,...,1\rangle\langle 111,...,1}$ is successfully achieved. In this proposed protocol, to keep the indistinguishability (coherence) of the transmitted (Eq. (10)) and reflected (Eq. (11)) pulses, the product of the single photon pulse length and the coupling constant g should be much larger than 1 [9]. Moreover, the pulse length should be much longer than the distance between first and last atom.

The above method is also valid where N atoms are separated in N sections of the waveguide. If the relative phase differences induced by the optical distances between neighboring atoms $d_{i-1,i}$ are integer multiples of 2π and $\sum_{i=2}^{N} d_{i-1,i}$ is much shorter than the pulse length, the interaction result is still the same with that all of atoms in one waveguide (Eq. (9)). By external and deterministic control of the coupling of single atom-waveguide subsystems (shown in Fig. 4(d) as the ith unit) to the main bus waveguide, the multi-atom CPF gate can be realized among any of the N atoms. Because there is no entanglement between the N atoms and the single photon after interaction in the Sagnac interferometer, the multi-atom CPF gate can be achieved without detecting the photon. However, photon loss induced by atomic decay will decrease the success probability and gate fidelity. As an example, the two-atom state $(|0\rangle + |1\rangle)/\sqrt{2} \otimes (|0\rangle + |1\rangle)/\sqrt{2}$ under the interaction will be transformed to $((P_1 + P_2 - 1)/(P_1 + P_2 + 1)|00\rangle + (P_1 - 1)/(P_1 + 1)|01\rangle + (P_2 - 1)/(P_2 + 1)|10\rangle - |11\rangle)/2\sqrt{S_2}$, where the normalization coefficient S_2 is the success probability. S_2 is described as $(|(1 - P_1 - P_2)/(1 + P_1 + P_2)|^2 + |(1 - P)/(1 + P)|^2 + |(1 - P_2)/(1 + P_2)|^2 + 1)/4$. Correspondingly, the fidelity of the two-atomic CPF gate is $F_2 = |(P_1 + P_2 - 1)/(P_1 + P_2 + 1) + (P_1 - 1)/(P_1 + 1) + (P_2 - 1)/(P_2 + 1) + 1|/4\sqrt{S_2}$. Fig. 6 shows the success probability and gate fidelity for different effective Purcell factors for the resonant cases ($\upsilon = \omega_1 = \omega_2$). We assume that the atoms have the same transition frequency and effective Purcell factor. In Fig. 6(b), the fidelity can achieve as high as 99.9% for $P_1 = P_2 = 20$, an effective Purcell factor which is not difficult to obtain in nanowire surface plasmons [7,18] or PhC waveguide [6,20]. For example, in the nanowire surface plasmons, the effective Purcell factor can exceed 10^3 [18]. Moreover, slight difference of the two effective Purcell factors does not influence the success probability and fidelity much, as shown in Fig. 6. For the multi-atom CPF gate with the same effective Purcell factors P_0, the success probability is $S_N = \sum_{k=0}^{N} N!/k!(N-k)!(1 - kP_0/1 - kP_0)^2 / \sum_{k=0}^{N} N!/k!(N-k)!$, and the fidelity is $F_N = [\sum_{k=1}^{N} N!/k!(N-k)!(1 - kP_0/1 - kP_0)]/\sqrt{S_N}\sum_{k=0}^{N} N!/k!(N-k)!$. The success probability and fidelity are much higher (as shown in the insets of Fig. 6 for 10 atoms) because of the coherent superposition, leading to a higher $P = \sum_l P_l$.

We proposed and examined the interaction between a single photon and N atoms in a one-dimensional waveguide embedded in a Sagnac interferometer. The relationship of the input and output mode is obtained by solving the dynamical equations. The result can also be achieved through transfer matrices [21,19]. The result in Eq. (9) can be rewritten as a transfer matrix [10], which can be decomposed as the product of N transfer matrices of single-photon and single-atom interactions.

4. Conclusion

In summary, we have proposed a new scheme to realize quantum control phase-flip gate between two

photons through photon–QD interaction in a PhC waveguide. Strong optical confinement and low group velocity in PhC waveguide contributes to the high gate fidelity (∼0.99) over a tremendous broadband region (2 THz). Moreover, the multi-atom CPF gate is constructed in the Sagnac interferometer with high fidelity in only one step. The proposed two-side input coupling method, with the beam splitter and the Sagnac interferometer, distinctively erases the entanglement between the atom and photon and transforms atoms into the demanded state without detecting the photon. By controlling the coupling between different single atom-embedded waveguide subsystems to a main waveguide, the atomic cluster state [22,23,24] can be generated, which is the fundamental element for one-way quantum computation [23,24]. Excitation and extraction can be extremely efficient and chip-scale integration is possible. All these advantages show QD–PhC waveguide system is very promising to be a critical component in quantum information processing.

Acknowledgements

The authors thank J.-T. Shen, S. Fan and X.D. Yang for helpful discussions. We acknowledge funding support from the 2008 National Science Foundation CAREER Award (NSF ECCS 0747787), the 2007 DARPA Young Faculty Award, and the New York State Office of Science, Technology and Academic Research.

References

[1] J. McKeever, A. Boca, A.D. Boozer, R. Miller, J.R. Buck, A. Kuzmich, H.J. Kimble, Science 303 (2004) 1992.
[2] Y.F. Xiao, J. Gao, X. Yang, R. Bose, G.C. Guo, C.W. Wong, Appl. Phys. Lett. 91 (2007) 151105.
[3] L.-M. Duan, H.J. Kimble, Phys. Rev. Lett. 92 (2004) 127902.
[4] E. Waks, J. Vuckovic, Phys. Rev. Lett. 96 (2006) 153601.
[5] S.J. Devitt, A.D. Greentree, R. Ionicioiu, J.L. O'Brien, W.J. Munro, L.C.L. Hollenberg, Phys. Rev. A 76 (2007) 052312.
[6] V.S.C. Manga Rao, S. Hughes, Phys. Rev. B 75 (2007) 205437.
[7] D.E. Chang, A.S. Sorensen, E.A. Demler, M.D. Lukin, Nat. Phys. 3 (2007) 807.
[8] E. Viasnoff-Schwoob, C. Weisbuch, H. Benisty, S. Olivier, S. Varoutsis, I. Robert-Philip, R. Houdre, C.J.M. Smith, Phys. Rev. Lett. 95 (2005) 183901.
[9] W. Langbein, P. Borri, U. Woggon, V. Stavarache, D. Reuter, A.D. Wieck, Phys. Rev. B 70 (2004) 033301.
[10] J.T. Shen, S. Fan, Opt. Lett. 30 (2005) 15.
[11] Y. Tanaka, J. Upham, T. Nagashima, T. Sugiya, T. Asano, S. Noda, Nat. Mater. 6 (2007) 862.
[12] R.A. Campos, B.E.A. Saleh, M.C. Teich, Phys. Rev. A 40 (1989) 1371.
[13] J.I. Cirac, P. Zoller, H.J. Kimble, M. Mabuchi, Phys. Rev. Lett. 78 (1997) 3221.
[14] A.V. Gorshkov, A. Andre, M. Fleischhauer, A.S. Sorensen, M.D. Lukin, Phys. Rev. Lett. 98 (2007) 123601.
[15] A.D. Boozer, A. Boca, R. Miller, T.E. Northup, H.J. Kimble, Phys. Rev. Lett. 98 (2007) 193601.
[16] E. Kuramochi, M. Notomi, S. Mitugi, A. Shinya, T. Tanabe, T. Watanabe, Appl. Phys. Lett. 88 (2006) 041112.
[17] D.F. Walls, G.J. Milburn, Quantum Optics, Springer–Verlag, Berlin, 1994.
[18] D.E. Chang, A.S. Sorensen, P.R. Hemmer, M.D. Lukin, Phys. Rev. B 76 (2007) 035420.
[19] J.-T. Shen, M.L. Povinelli, S. Sandhu, S. Fan, Phys. Rev. B 75 (2007) 035320.
[20] V.S.C. Manga Rao, S. Hughes, Phys. Rev. Lett. 99 (2007) 193901.
[21] P. Yeh, Optical Waves in Layered Media, John Wiley & Sons, New York, 1988.
[22] H.J. Briegel, R. Raussendorf, Phys. Rev. Lett. 86 (2001) 910.
[23] R. Raussendorf, H.J. Briegel, Phys. Rev. Lett. 86 (2001) 5188.
[24] R. Raussendorf, D.E. Browne, H.J. Briegel, Phys. Rev. A 68 (2003) 022312.